Hydrolysis and Radiation Chemistry of the DGAs

Fuel Cycle Research & Development

Prepared for
U.S. Department of Energy
Materials Recovery and Waste Form Development Campaign

Bruce J. Mincher and Christopher A. Zarzana
National Laboratory

15 Sept. 2016

FCRD-MRWFD-2016-000369

SUMMARY

This document was prepared to meet FCR&D level 3 milestone M3FT-16IN030104052, "continue the study of the short chain compounds," and, " study the radiolysis of the non-symmetrical DGA (D_3DODGA)…," under the Radiation Chemistry FCR&D work package. Toward these goals, the short chain DGA, tetraethyldiglycolamide (TEDGA) was investigated for its hydrolytic stability in HNO_3 solution, with comparisons to the less oxidizing mineral acid HCl. Initial gamma-irradiations were also performed on DGA solutions, to inform a more detailed investigation of several short chain compounds anticipated for FY17. The hydrolytic and radiolysis behavior of TEDGA is of interest for two reasons. First, previous long chain DGA radiolysis was conducted in dodecane solution since the long chain compounds are soluble in that diluent, and new radiation chemistry is expected in the aqueous environment due to reactions with $^{\bullet}$OH radical. The second reason is that this water-soluble DGA has been proposed for use as a stripping or holdback agent in both European and American fuel cycle scenarios. Therefore, this work was performed in collaboration Forschungszentrum Jülich (FZJ), and the European SACSESS program. Additionally, results are presented here regarding the radiation of chemistry the non-symmetrical DGA didodecyldioctyldiglycolamide (D_3DODGA), for comparison to previous work with symmetrical DGAs such as TODGA and TEHDGA. This was also conducted in collaboration with researchers in the SACSESS program.

CONTENTS

ACRONYMS

ACS	American Chemical Society
ALSEP	Actinide Lanthanide SEParation process
CHON	Carbon, Hydrogen, Oxygen, Nitrogen
D_3DODGA	didodecyldicotyldiglycolamide
DGA	diglycolamide
ESI	Electrospray Ionization
FZJ	Forschungszentrum Jülich
HLW	High Level Waste
INL	Idaho National Laboratory
LC/MS	Liquid Chromatography/Mass Spectrometry
MeTEDGA	methyltetraethyldiglycolamide
Me_2TEDGA	dimethyltetraethyldiglycolamide
MeTODGA	methyltetraoctyldiglycolamide
Me_2TODGA	dimethyltetraoctyldiglycolamide
SACSESS	Safety of ACtinide SEparation procesSeS
TEDGA	tetraethyldiglycolamide
TEHDGA	teraethylhexyldiglycolamide
TODGA	tetraocyldiglycolamide
TOF	Time of Flight
UK	United Kingdom
UHPLC	Ultra High Performance Liquid Chromatography

DGA HYDROLYSIS AND RADIOLYSIS

1. INTRODUCTION

One class of molecules that has received much attention in the last decade as candidate extractants for lanthanides and actinides is the tetraalkyldiglycolamides (DGAs). These compounds exhibit excellent extraction efficiency for the trivalent *f*-elements and contain only carbon, hydrogen, oxygen, and nitrogen (CHON); they can be easily incinerated, reducing the volume of waste generated from reprocessing. When their N-alkyl substituents are varied, it is found that long chain derivatives have decreased solubility in water and increased solubility in aliphatic hydrocarbon diluents such as *n*-dodecane. [1] Short chain compounds are water soluble, and have been used as aqueous stripping and hold back agents in both European and American proposals. For example, the American ALSEP (Actinide Lanthanide Separation) process uses the branched DGA *N,N,N',N'*-tetra(ethylhexyl)digylcolamide (TEHDGA) as the organic-phase extractant, and the water soluble tetraethyldiglycolamide (TEDGA) as a lanthanide stripping agent. [2]

Of the hydrophobic DGAs, *N,N,N',N'*-tetraoctyldiglycolamide (TODGA) has received the most attention for use in the back end of the nuclear fuel cycle, as it is freely soluble in *n*-dodecane with high americium distribution ratios. The branched TEHDGA has also been investigated as a cheaper alternative to TODGA, although TEHDGA has lower distribution ratios. However, it also extracts lower amounts of fission products while maintaining acceptable *f*-element extraction efficiency. Methyl-substituted TODGAs such as MeTODGA and Me_2TODGA have also been explored for the same reason. [3] These studies indicate that the N-alkyl substituents play a significant role in the hydrophilicity, lipophilicity, and extraction behavior of DGAs.

Because of the high concentrations of metal ions in high-level waste (HLW), candidate separation processes must be robust against third-phase formation. Unfortunately, TODGA and TEHDGA form third-phases in paraffinic diluents at low (millimolar) metal concentrations. Thus, all processes using DGAs that have been tested with simulated or actual HLW have used phase modifiers. While phase modifiers such as TBP can successfully suppress third-phase formation, their use can increase the overall cost and complexity of a separation process and defeat the purpose of a CHON compliant ligand. Therefore, the development of alternative DGAs with asymmetrical side chains has been performed. Compounds such as di-dodecyl-di-octyldiglycolamide (D_3DODGA) have high distribution ratios for trivalent lanthanides and actinides, low distribution ratios for strontium, and no third phase formation with high metal loading. [4]

An understanding of the influence of radiation from HLW on separation ligands is critical to the development and implementation of robust separation processes. Additionally, the influence of acid hydrolysis is important for water-soluble ligands. Here, an investigation of the radiolysis of D_3DODGA was performed, including measurements of the dose constants for degradation of the parent compound, and the ingrowth of degradation products. Initial investigations of the hydrolysis and radiolysis of TEDGA are also reported. These efforts were conducted in collaboration with researchers at Forschungszentrum Jülich (FZJ), under the auspices of the European SACSESS program.

2. EXPERIMENTAL

2.1 Reagents

The TEDGA was supplied by Technocom (UK) and used as received. The D^3DODGA was synthesized and supplied by FZJ, and used as received. All other reagents were ACS reagent grade.

2.2 Hydrolysis and Radiolysis

Irradiations were performed at INL using a Nordion Gammacell 220, at a dose rate of 4–4.5 kGy h^{-1}, depending on the date of irradiation, as initially measured using standard Fricke procedures, and then subsequently corrected for ^{60}Co decay. The TEDGA solutions were irradiated either as a 0.05 M solution in nanopure water, and 0.05 M in 2.5 M HNO_3 to absorbed doses of 0, 100, 250 and 400 kGy, in sealed containers.

Hydrolysis experiments were run on 1 M solutions of TEDGA in 0.5 and 4.0 M HNO_3 at 25ºC, 35ºC, 45ºC, 55ºC and 65ºC; and in 5.0 or 8.0 M HCl at 65ºC. Immediately after the sample was prepared a T_0 sample was collected and then the sampling was continued for an appropriate period of time, with the samples in a temperature controlled environment between sampling events.

The D^3DODGA was irradiated as nominally 0.05 M solutions in dodecane. Aliquots of these solutions were irradiated as the pure organic phase, or in contact with 2.5 M HNO_3, both with and without air sparging to ensure the presence of dissolved oxygen in the sparged samples. Sparging was conducted at an air flow rate of 1 mL min^{-1}, using a needle inserted through the septum of the sample container, with a second needle inserted to release the air flow to atmosphere. Flow was controlled by a mass flow controller with the flow rate selected to ensure no evaporation losses in the sample volume but sufficient to provide a reasonable expectation of air saturation in the 5 mL samples.

2.3 Mass Spectrometry

The TEDGA samples were diluted in 50:50 H_2O:Optima® LC/MS acetonitrile (Fisher Scientific, Pittsburg, PA) prior to analysis in order to generate a concentration in the low micromolar (μM) range (i.e., in the middle of the response versus concentration curve). The diluted samples were analyzed using a Dionex (Sunnyvale, CA) ultra-high-performance liquid chromatograph (UHPLC) with an Ultimate 3000 RS pump, 3000 RS autosampler, 3000 RS column compartment and a 3000 RS diode array detector, coupled to a Bruker (Billerica, MA) microTOFQ-II electrospray ionization quadrupole time-of-flight mass spectrometer with Hystar 3.2 software.

Irradiated D_3DODGA samples in were diluted in Optima® LC/MS 2-propanol (Fisher Scientific, Pittsburg, PA) prior to analysis in order to generate a concentration in the low micromolar (μM) range (i.e., in the middle of the response versus concentration curve). TODGA served as an internal standard. Calibration standards were constructed from the analyses of a primary solution of D_3DODGA solutions generated gravimetrically. All of the diluted samples and calibration solutions were analyzed using a Dionex (Sunnyvale, CA) ultra-high-performance liquid chromatograph (UHPLC) with an Ultimate 3000 RS pump, 3000 RS autosampler, 3000 RS column compartment and a 3000 RS diode array detector, coupled to a Bruker (Billerica, MA) microTOFQ-II electrospray ionization quadrupole time-of-flight mass spectrometer with Hystar 3.2 software.

3. RESULTS AND DISCUSSION

3.1 Hydrolysis of TEDGA

The change in TEDGA concentration versus acid contact time for samples prepared in 0.5 M HNO_3 and 4.0 M HNO_3 at 5 different temperatures is shown in Fig. 1 and the corresponding rate constants (k) for each system are shown in Table 1.

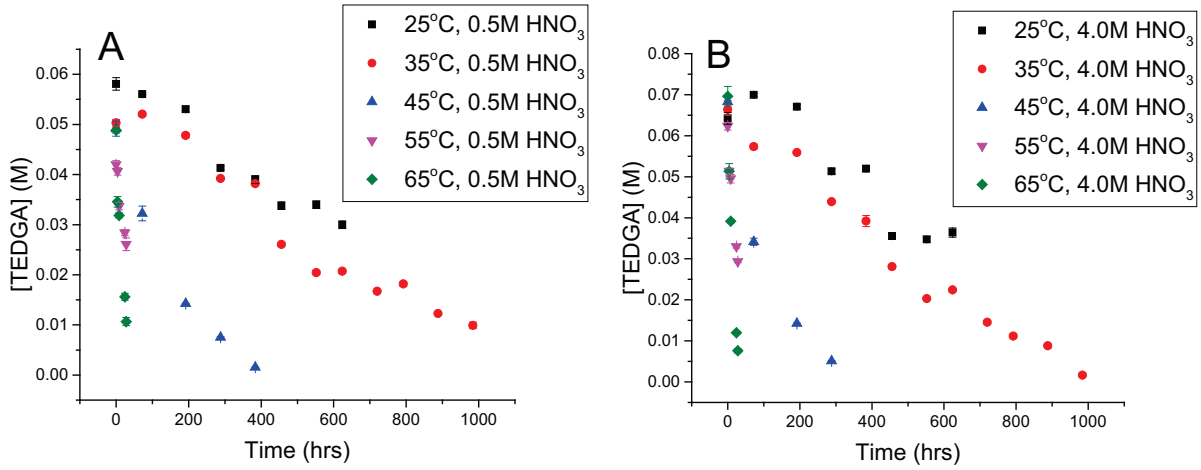

Figure 1. TEDGA concentration vs. acid contact time for both the 0.5 M HNO_3 (A) and 4.0 M HNO_3 (B) samples. The solid black squares are at 25°C; solid red circles are at 35°C; solid blue triangles are at 45°C; solid pink triangles are at 55°C; solid green diamonds are at 65°C. Each point is the mean of five measurements and the error bars represent 99% confidence intervals.

Table 1. Measured rate constants (h^{-1}) for the degradation of TEDGA at the five temperatures studied. The rate constants were calculated from linear fits of plots of ln[TEDGA] vs. acid contact time.

Sample	Rate Constant k (h^{-1})
25°C, 0.5 M HNO_3	$(1.1 \pm 0.2) \times 10^{-3}$
35°C, 0.5 M HNO_3	$(1.7 \pm 0.2) \times 10^{-3}$
45°C, 0.5 M HNO_3	$(8.5 \pm 1.3) \times 10^{-3}$
55°C, 0.5 M HNO_3	$(1.7 \pm 0.4) \times 10^{-2}$
65°C, 0.5 M HNO_3	$(5.0 \pm 0.6) \times 10^{-2}$

25°C, 4.0 M HNO_3	$(1.2 \pm 0.3) \times 10^{-3}$
35°C, 4.0 M HNO_3	$(2.3 \pm 0.2) \times 10^{-3}$
45°C, 4.0 M HNO_3	$(8.8 \pm 0.5) \times 10^{-3}$
55°C, 4.0 M HNO_3	$(2.5 \pm 0.3) \times 10^{-2}$
65°C, 4.0 M HNO_3	$(7.8 \pm 0.6) \times 10^{-2}$
65°C, 5.0 M HCl	$(7.0 \pm 0.4) \times 10^{-2}$
65°C, 8.0 M HCl	$(5.2 \pm 0.2) \times 10^{-2}$

Also shown in Table 1 are TEDGA hydrolysis data for HCl at 65°C. It can be seen that the degradation rate constants are similar for the two acids at 4–5 M in acid at that temperature, suggesting that the reaction is acid hydrolysis rather than oxidation. Interestingly, the rate appears to decrease for increasing [HCl], in contrast to what was observed for HNO_3, suggesting that oxidation may become more important with increasing [HNO_3].

3.2 Initial Radiolysis of TEDGA

Solutions of nominally 0.05 M TEDGA were prepared in water, and in 2.5 M HNO_3, and irradiated over a series of absorbed doses to 400 kGy maximum. The TEDGA concentration was then measured by mass spectrometry. The results are shown in Fig. 2 (left).

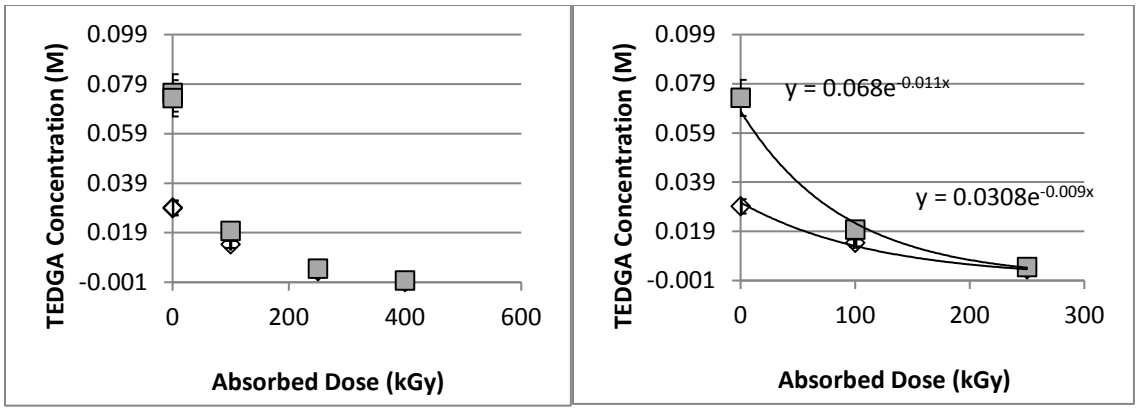

Figure 2. TEDGA concentration vs. absorbed dose for irradiaton in water (shaded boxes) and 2.5 M HNO_3 (open diamonds). Full data set (left) and exponential fit used to calculate dose constant (right).

It can be seen in Fig 2 that the decrease in [TEDGA] is exponential, in agreement with kinetics seen for the DGAs in organic solution. The data at 400 kGy are at or below detection limit,

consequently the data were replotted in Fig. 2 (right). The exponential fit to the water irradiation data provides a dose constant of 0.011 kGy^{-1}. This degradation rate is about a factor of three higher than that reported for organic-soluble DGAs (see Section 3.3 below).

Also shown in Fig. 2 are similar data for TEDGA irradiation in 2.5 M HNO_3, which results are also exponential. However, as can be seen especially in the initial unirradiated sample, the initial concentration is lower than expected, presumably due to TEDGA hydrolysis. Based on the room temperature hydrolysis rate constants shown in Table 1, it would be predicted that the initial TEDGA concentration in the acidic sample would be even lower given the elapsed time between irradiation and analysis; however, the samples were stored under refrigeration. Although an exponential constant can be obtained from the fit to the acid data, it is not reported as a dose constant here since it is the result of both radiolysis and hydrolysis.

Based on this scoping irradiation, FY17 work should include irradiation to < 200 kGy, with an immediate sample dilution after irradiation. A control set that is unirradiated should be treated identically. They would be chilled and transported for analysis directly after irradiation. This will be performed for TEDGA, TMDGA, Me-TEDGA, and ME_2-TEDGA, in collaboration with FZJ.

3.3 Radiolysis of D_3DODGA

The detailed results for the irradiation studies of D^3DODGA were published in the manuscript entitled, "A study of the γ-radiolysis of di-dodecyl di-octyl diglycolamide using UHPLC-ESI-MS analysis," by Roscioli-Johnson et al. [5] That paper is attached here (author-accepted version) as Appendix A. Therefore, only a brief review is provided in this report.

The change in D_3DODGA concentration versus absorbed γ-dose for samples irradiated as the organic phase or in contact with 2.5 M HNO_3 both with and without sparging is shown in Fig 3. The concentration change versus absorbed dose data may be fit with an exponential curve, suggesting pseudo-first-order kinetics, probably a reaction with a direct radiolysis product of the diluent. The degradation rate is identical under all investigated conditions, with a mean dose constant (*d*) of (3.9 ± 0.3) x 10^{-3} kGy^{-1}. This is comparable to the dose constant reported by Zarzana et al. for TODGA/TEHDGA of (4.1 ± 0.3) x 10^{-3} kGy^{-1}, [6] and slightly lower than the dose constants reported by Galán et al. for MeTODGAs of ~ 5 x 10^{-3} kGy^{-1}. [7] Both previous studies were also conducted under this program. The rate appears to be unaffected by contact with nitric acid and air sparging; a finding also in agreement with studies of the other lipophilic DGAs. [6,7]

Products analysis indicated that there is a difference in degradation chemistry that depends on whether the organic phase is in contact with acid; in the presence of an acidic aqueous phase, the preferred site for radiolytic attack appears to be at the amide nitrogen atoms, which produces a higher fraction of products generated from rupture of the N–$C_{carbonyl}$ and the N–C_{alkyl} bonds. The C–O_{ether} and C–$C_{carbonyl}$ bonds are also broken, but

these reactions account for a greater fraction of the overall reactivity in the non-acid-contacted experiments. This suggests that acid contact may degrade separation efficiency via production of new complexing agents, and that further study to evaluate this possibility is warranted.

There is also a striking similarity in the degradation pathway of the D_3DODGA [5] when compared to the degradation of TODGA, and TEHDGA, [6] and MeTODGA and Me_2TODGA. [7] The similarity in degradation rates of these DGA compounds, along with the identified radiolysis products discussed above, strongly suggests that the diglycolamide center of these molecules, not the side-chains, is most vulnerable to radiolytic degradation, apparently all by reaction with a common species produced by radiolysis of the organic phase.

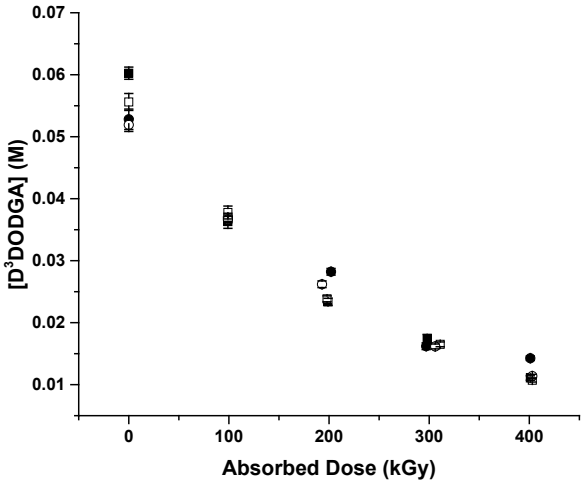

Figure 3. D_3DODGA concentration vs. absorbed dose. The solid squares are 0.05 M D_3DODGA organic phase; the open squares are 0.05 M D_3DODGA air sparged organic phase; the solid circles are 0.05 M D_3DODGA organic phase contacted with 2.5 M HNO_3; the open circles are 0.05 M D_3DODGA air sparged organic phase contacted with 2.5 M HNO_3. Each point is the mean of five measurements and the error bars represent 99% confidence intervals.

4. CONCLUSION AND FUTURE WORK

All the investigated lipophilic DGAs degrade by a common mechanism under radiolysis, to provide predictable products. Rupture of the ether linkages predominates, regardless of alkyl substitution. Under acid conditions C–N bond breakage becomes more common, to produce new complexing agents. The kinetics of degradation is pseudo first order, and the rate constant is approximately the same for each compound. In initial measurements of the radiolysis of the water soluble TEDGA in aqueous solution, the kinetics was also first order and the rate constant was about 3x faster. The TEDGA is also susceptible to acid hydrolysis, with increasing rates at elevated temperature and nitric acid concentration. Based on this scoping irradiation, FY17 work should include irradiations with an immediate sample dilution after irradiation to mitigate

hydrolysis. A control set that is unirradiated will be treated identically. They will be chilled and transported for analysis directly after irradiation. This will be performed for TEDGA, TMDGA, Me-TEDGA, and ME_2-TEDGA, in collaboration with FZJ.

5. REFERENCES

1. Sasaki, Y.; Sugo, Y.; Morita, K.; Nash, K.L. 2015. The effect of alkyl substituents on actinide and lanthanide extraction by diglycolamide compounds. *Solvent Extr. Ion Exch*. 33: 625-641.

2. Moyer, B.A.; Lumetta, G.L.; Mincher, B.J. Minor actinide separation in the reprocessing of spent nuclear fuel: recent advances in the United States, Ch. 11 in: Taylor, R. Reprocessing and recycling of Spent Nuclear Fuel. Woodhead Publishing Series in Energy, Number 79, Elsevier, NY, 2015.

3. Wilden, A.; Modolo, G.; Lange, S.; Sadowski, F.; Beele, B.B.; Skerencak-Frech, A.; Panak, P.J.; Iqbal, M.; Verboom, W.; Geist, A.; Bosbach, D. 2014. Modified diglycolamides for the Am(III) + Ln(III) Co-separation: Evaluation by solvent extraction and time-resolved laser fluorescence spectroscopy. *Solvent Extr. Ion Exch*. 32:119-137.

4. Ravi, J.; Venkatesan, K. A.; Antony, M. P.; Srinivasan, T. G.; Vasudeva Rao, P. R. 2014. Feasibility of Using Di-Dodecyl-Di-Octyl Diglycolamide for Partitioning of Minor Actinides from Fast Reactor High-Level Liquid Waste. *Solvent Extr. Ion Exch*. 32: 424–436.

5. Roscioli-Johnson, K.M.; Zarzana, C.A.; Groenewold, G.S.; Mincher, B.J.; Wilden, A.; Schmidt, H.; Modolo, G. A study of the γ-radiolysis of di-dodecyl di-octyl diglycolamide using UHPLC-ESI-MS analysis. *Solvent Extr. Ion Exch*. DOI: 10.1080/07366299.2016.1212540.

6. Zarzana, C.A.; Groenewold, G.S.; Mincher, B.J.; Mezyk, S.P.; Wilden, A.; Schmidt, H.; Modolo, G.; Wishart, J.F.; Cook, A.R. 2015. A comparison of the γ-radiolysis of TODGA and T(EH)DGA using UHPLC-MS analysis. *Solvent Extr Ion Exch* 33:431-447.

7. Galán, H.; Zarzana, C.A.; Wilden, A.; Núñez, A.; Schmidt, H.; Egberink, R.J.M.; Leoncini, A.; Cobos, J.; Verboom, W.; Modolo, G.; Groenewold, G.S.; Mincher, B.J. 2015. Gamma-radiolytic Stability of New Methylated TODGA Derivatives for Minor Actinide Recycling. *Dalton Trans* 44:18049-18056.

Appendix A

D_3DODGA MANUSCRIPT

A STUDY OF THE Γ-RADIOLYSIS OF *N*,*N*-DI-DODECYL-*N'*,*N'*-DI-OCTYLDIGLYCOLAMIDE (D^3DODGA) USING UHPLC-ESI-MS ANALYSIS

Kristyn M. Roscioli-Johnson[a], Christopher A. Zarzana*[a], Gary S. Groenewold[a], Bruce J. Mincher[a], Andreas Wilden[b], Holger Schmidt[b], Giuseppe Modolo[b], Beatrix Santiago-Schübel[c]

3. Abstract:

Solutions of *N*,*N*-di-dodecyl-*N'*,*N'*-di-octyldiglycolamide in *n*-dodecane were subjected to γ irradiation in the presence and absence of both an aqueous nitric acid phase and air sparging. The solutions were analyzed using UHPLC-ESI-MS to determine the rates of radiolytic decay of the extractant, as well as to identify radiolysis products. The DGA concentration decreased exponentially with increasing dose, and the measured degradation rate constants were uninfluenced by the presence or absence of acidic aqueous phase, or by air sparging. The identified radiolysis products suggest that the bonds most vulnerable to radiolytic attack are those in the diglycolamide center of these molecules and not in the side chains.

a Idaho National Laboratory, 2525 Fremont Ave., Idaho Falls, ID 83415-2208, United States.

* Address reprint requests to Christopher A. Zarzana, Idaho National Laboratory, 775 University Boulevard, Idaho Falls, ID 83415-3531, United States. E-mail: christopher.zarzana@inl.gov

b Forschungszentrum Jülich GmbH, Institut für Energie- und Klimaforschung- Nukleare Entsorgung und Reaktorsicherheit (IEK-6), 52428 Jülich, Germany.

c Forschungszentrum Jülich GmbH, Zentralinstitut für Engineering, Elektronik und Analytik (ZEA-3), 52428 Jülich, Germany.

4. Introduction

The safe processing and disposal of spent nuclear fuel is a major step required for the wide-spread use of nuclear power. However, the radiotoxicity of untreated spent fuel requires several hundred thousand years to decay to the level of natural uranium ore, presenting a significant challenge for secure, long-term disposal. Long-lived radioisotopes of plutonium, and the minor actinides neptunium, americium and curium make up the bulk of nuclides responsible for the thermal heat load and radiotoxicity past several hundred years.[1–4] Thus, separation of these constituents from the rest of the fission products (partitioning) followed by burning in a fast nuclear reactor (transmutation) can dramatically reduce the storage requirements for spent nuclear fuel. In fact, by reducing waste heat production a more efficient utilization of the repository is likely. These are important issues to ensure the future sustainability of nuclear power.

One class of molecules that has received much attention in the last decade as candidate extractant for lanthanides and actinides is the diglycolamides (DGAs).[5] These molecules are of interest because they exhibit higher Am(III) affinity than extractants such as octyl-(phenyl)–*N*,*N*-diisobutyl carbamoyl methyl phosphine oxide (CMPO) from solutions with nitric acid concentrations in the range found in high-level waste (HLW).[6] Additionally, because DGAs contain only carbon, hydrogen, oxygen, and nitrogen (CHON), they can be easily incinerated, reducing the volume of secondary waste generated from reprocessing used nuclear fuel. Sasaki et al. synthesized a series of diglycolamides, varying their *N*-alkyl substituents (alkyl = C_nH_{2n+1} with n = 3, 4, 5, 6, 8 and 10) and found that as n increased, solubility in water decreased, solubility in alphatic hydrocarbon diluents such as *n*-dodecane increased, and the americium distribution ratio (extraction from 1 M HNO_3 by 0.1 M DGA) decreased.[7] Mowafy and Aly synthesized a series of DGAs with straight and branched *N*-alkyl substituents and obtained similar

results.[8] These studies indicate that the *N*-alkyl substituents play a significant role in the hydrophilicity, lipophilicity, and extraction behavior of DGAs.

Of the DGAs, *N,N,N',N'*-tetraoctyldiglycolamide (TODGA) has received the most attention for actinide partitioning within the back end of the nuclear fuel cycle, as it is freely soluble in *n*-dodecane with high americium distribution ratios from strong nitric acid medium. The branched DGA *N,N,N',N'*-tetra(2-ethylhexyl)digylcolamide (T(EH)DGA) has also been investigated as an alternative to TODGA, with lower affinity towards trivalent actinides and for some undesirable fission products. Because of the high concentrations of metal ions and HNO_3 acidity in HLW, candidate separation processes must be robust against third-phase formation. Third-phase formation occurs when the organic phase splits into two distinct phases (a metal-rich phase and a diluent-rich phase), an undesirable condition for industrial-scale solvent extraction. The Limiting Organic Concentration (LOC) is the maximum concentration of metal ions that can be loaded into the organic phase without third-phase formation. Unfortunately, TODGA and TEHDGA form third-phases in paraffinic diluents at low (millimolar) metal concentrations and thus will suffer from third-phase formation when used with HLW. Studies of third-phase formation of DGA/*n*-dodecane organic phases have found that the LOC for Nd increased with temperature, DGA concentration, and *N*-alkyl chain length.[9–11] However, an increase in TODGA concentration also increased the extraction of HNO_3 which would impede back-extraction. Addition of *N,N*-dihexyl-octanamide (DHOA) as a phase modifier increased the LOC. Thus, all processes using DGAs that have been tested with simulated or actual HLW have used phase modifiers. For example, a process developed at Forschungszentrum Jülich used 0.2 M TODGA modified with 0.5 M tri-*n*-butyl phosphate (TBP) in the industrial alkane diluent hydrogenated tetrapropene (TPH) to extract Eu^{III}, Am^{III}, Cm^{III}, Cf^{III}, and Th^{IV} from simulated high level raffinates with nitric acid concentrations from 1–3 M.[12–14] The TBP acted as an extractant and a phase-modifier, mitigating third-phase formation. However, oxalic acid and *N*-(2-hydroxyethyl)-ethylenediamine-triacetic acid (HEDTA) were required to mitigate the co-extraction of zirconium, molybdenum, and palladium.

While phase modifiers can successfully suppress third-phase formation, their use can increase the overall cost and complexity of a separation process; therefore, it is desirable to develop alternative extractants that are resilient to third-phase formation without the use of phase modifiers. For symmetric DGAs (all four *N*-alkyl groups are the same), extraction strength decreases and resistance to third phase formation increases as the alkyl chain length increases. Ravi et al. suggested that a DGA with side groups with two different lengths would result in a DGA which had a combination of the properties of the two associated symmetric DGAs.[15] Using this idea, researchers at the Indira Gandhi Center for Atomic Research Kalpakkam developed the new unsymmetrical 2-(2-(didodecylamino)-2-oxoethoxy)-N,N-dioctylacetamide (trivially *N*,*N*-di-dodecyl-*N'*,*N'*-di-octyldiglycolamide, D^3DODGA, Figure 1) as a potential modifier-free actinide extractant.[16–19] They found that D^3DODGA had high distribution ratios for trivalent lanthanides and actinides (D_M > 300 for 3–8 M HNO_3), low distribution ratios for strontium, and no third phase formation was observed in 3–4 M HNO_3 solutions. Systematic variation of the non-*n*-didodecyl side chains suggested the presence of the di-docdecyl side chains were sufficient to prevent third-phase formation.[20] Extraction experiments using simulated fast-reactor high-level liquid waste showed 0.1 M D^3DODGA in *n*-dodecane had similar performance to TODGA-based systems without requiring a phase modifier.[17] Addition of trans-1,2-diaminocyclohexane-*N*,*N*,*N'*,*N'*-tetraacetic acid (CDTA) helped prevent the co-extraction of zirconium and palladium.[21]

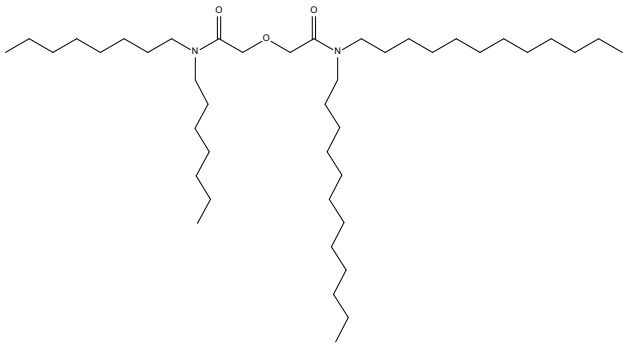

Figure 1: Structure of the diglycolamide studied here: di-dodecyl di-octyl diglycolamide (D^3DODGA).

Solvent extraction systems for partitioning used nuclear fuel will be exposed to high radiation fields and highly acidic conditions; therefore, the radiolytic and hydrolytic stability of extractant molecules is of interest for the development of robust separation processes. Prior research indicates that the long-chain DGAs are hydrolytically stable but vulnerable to radiolytic degradation.[12,22–31] Investigation of DGA radiolysis in *n*-dodecane suggest that the most vulnerable bonds are those within the diglycolamide functional group, specifically the C–O_{ether}, N–$C_{carbonyl}$ and the N–$C_{side\text{-}chain}$ bonds, and to a lesser extent the C-$C_{carbonyl}$ bond.[22,24–26] Neither Zarzana et al.[25] nor Sugo et al.[22] observed any influence from nitric acid contact on the radiolysis of TODGA and T(EH)DGA; however, Galán et al.[24] did report a protective effect due to nitric acid contact for TODGA. Additionally, compounds with one (MeTODGA) or two (Me_2TODGA) methyl groups added to the DGA backbone appeared to be more sensitive to radiolysis when contacted with nitric acid.[26]

At present, the only study of the radiolysis of D^3DODGA used changes in metal distribution ratios as a measure of DGA degradation.[30] However, prior studies of DGA degradation products indicated that radiolytically produced species can have significantly different extraction properties than the parent DGA;[24,28] thus, distribution ratios are an inappropriate measure of DGA degradation. In this article we present an investigation of the γ-radiolytic stability of D^3DODGA in *n*-dodecane using ultra-high performance liquid chromatography-electrospray ionization-mass spectrometry (UHPLC-ESI-MS) and high performance liquid chromatography/mass spectrometry (HPLC-HRMS) to directly monitor the

decrease in DGA concentration with absorbed dose and the generation of products. The irradiations were performed on the organic phase in the presence and absence of an aqueous nitric acid phase and with or without air sparging. While previous studies have examined the effect of an acidic aqueous phase on DGA radiolysis,[25,26] as a scavenger of many radiolytically-produced reactive species, dissolved oxygen is also important in radiation chemistry. However, gamma-radiolysis studies are usually conducted in sealed vessels in which dissolved oxygen is depleted in the first few Gy of absorbed dose, while the processes under which solvent extraction ligands are used are likely to be in contact with air.[27] Therefore, some D^{3}DODGA samples were also irradiated with continuous air sparging to ensure that dissolved oxygen was not depleted during the experiment.

5. Experimental

D^{3}DODGA was purchased from TechnoComm Ltd., Wellbrae, Scotland. All chemicals were of analytical grade and were used without further purification. Aqueous dilutions were done using ultrapure water (18.2 MΩcm).

GAMMA-RAY IRRADIATION

D^{3}DODGA was irradiated as nominally 0.05 M solutions in dodecane. Aliquots of these solutions were irradiated as the pure organic phase, or in contact with 2.5 M HNO_3. Samples with and without the presence of the aqueous phase were irradiated both with and without air sparging to ensure the presence of dissolved oxygen in the sparged samples. Sparging was conducted at an air flow rate of 1 mL min^{-1}, using a needle inserted through the septum of the sample container, with a second needle inserted to release the air flow to atmosphere. Flow was controlled by a mass flow controller with the flow rate selected to ensure no evaporation losses in the sample volume but sufficient to provide a reasonable expectation of air saturation in the 5 mL samples. Irradiations were conducted using a Nordion GammaCell 220E (Ottawa, Canada) ^{60}Co source, with a center-line sample chamber dose rate of 4.5 kGy h^{-1}, as determined by decay corrected Fricke dosimetry. Irradiation of the samples did not result in an elevated temperature.

UHPLC-ESI-TOF-MS

Irradiated D^3DODGA samples in *n*-dodecane were diluted in Optima® LC/MS 2-propanol (Fisher Scientific, Pittsburgh, PA) prior to analysis in order to generate a concentration in the low micro molar (μM) range (i.e., in the middle of the response versus concentration curve). At this point, 2.5 μL of a 100 μ M solution of TODGA was added; TODGA served as an internal standard. Calibration standards were constructed from the analyses of solutions of reagent grade D^3DODGA solutions; the primary standard was generated gravimetrically and secondary standards by serial dilution. Prior to analysis each serial standard was spiked with the TODGA internal standard, as described above. For each calibration standard, the ratios of the intensities of the D^3DODGA and TODGA protonated ions ($I_{D3DODGA}$ / I_{TODGA}) were multiplied by the TODGA concentration, and this value plotted versus the D^3DODGA concentration; the slope of the line of this plot was then used to calculate the D^3DODGA concentration in the experiments. All of the diluted samples and calibration solutions were analyzed using a Dionex (Sunnyvale, CA) ultra-high-performance liquid chromatograph (UHPLC) with an Ultimate 3000 RS pump, 3000 RS autosampler, 3000 RS column compartment and a 3000 RS diode array detector, coupled to a Bruker (Billerica, MA) microTOFQ-II electrospray ionization quadrupole time-of-flight mass spectrometer with Hystar 3.2 software.

The chromatographic separation was achieved using 5 μL injections on a Kinetex 1.3 μm particle size, C18 stationary phase, 50 mm × 2.1 mm column (Phenomenex, Torrance, CA, USA) held at 50 °C. The aqueous component was Optima® LC/MS water with 0.1% v/v formic acid (Fisher Scientific, Pittsburgh, PA), and the organic component was 3% v/v 1-octanol in Optima® LC/MS 2-propanol. A gradient mobile phase profile was used with a flow rate of 200 μL/min. The profile started at 50% organic for 5 min, followed by a 10 min ramp from 50% organic to 75% organic, followed by a hold at 75% organic for 10 min, and ending with a 1 min ramp back to 50% organic. The column was pre-equilibrated for 3 min at 50% organic before each injection. The mass spectrometer conditions were: capillary: 4.5 kV, positive mode; temp.: 220 °C; nebulizer gas and dry gas were both N_2, nebulizer pressure: 0.4 bar; dry gas flow

rate: 9 L/min. The mass spectrometer was operated using standard Bruker tuning parameters, specifically "tune low" (Table S1, Supplementary Information). Each sample was injected 5 times.

HPLC-APCI-FT-MS

HPLC-APCI-FT-MS measurements were performed at Forschungszentrum Jülich using a hybrid linear ion trap FTICR mass spectrometer LTQFT Ultra™ (Thermo Fisher Scientific, Bremen, Germany) coupled with an Agilent 1200 system (Agilent, Waldbronn, Germany). A ZORBAX Eclipse Plus C18, 4.6 × 100 mm, 3.4 µm (Agilent, Waldbronn) column was used with the following gradient: the gradient started with 60% B for 2 min, followed by a 8 min ramp from 60% B to 98% B followed by a hold of 98% B for 10 min and a re-equilibration of 10 min with 60% B. [(A: 0.1% v/v formic acid in H_2O), (B: 0.1% v/v formic acid in ACN)].

The mass spectrometer was used in the positive APCI mode. The MS conditions were: capillary temperature 275 °C, APCI vaporizer temperature: 400 °C, sheath gas flow 50, aux gas flow 5. The source voltage was 6kV, the capillary voltage 34 V and the tube lens 80V. Mass spectra were recorded in full scan from 100 to 1000 mass units with a resolution of 100,000 at *m/z* 400. All data were processed using the Xcalibur software version 2.0.

6. Results and Discussion

DEGRADATION OF D3DODGA AS A FUNCTION OF ABSORBED DOSE

The change in D^3DODGA concentration versus absorbed γ-dose for samples irradiated as the organic phase or in contact with 2.5 M HNO_3 both with and without sparging is shown in Figure 2. The concentration change versus absorbed dose data may be well fitted with an exponential curve, suggesting pseudo-first-order kinetics, probably a reaction with a direct radiolysis product of the diluent.[23] Dose constants (*d*) for each system are shown in Table 1, with the mean value for all conditions of $(3.9 \pm 0.3) \times 10^{-3}$ kGy^{-1}. This is comparable to the dose constants reported by Zarzana et al. for TODGA and TEHDGA of $(4.1 \pm 0.3) \times 10^{-3}$ kGy^{-1},[25] and slightly lower than the dose constants reported by Galán et

al. for methylated TODGA derivatives of ~ 5 x 10^{-3} kGy^{-1}.[26] As stated in previous work,[25] the *G*-value is not an appropriate metric because the decomposition of D^3DODGA occurs exponentially.

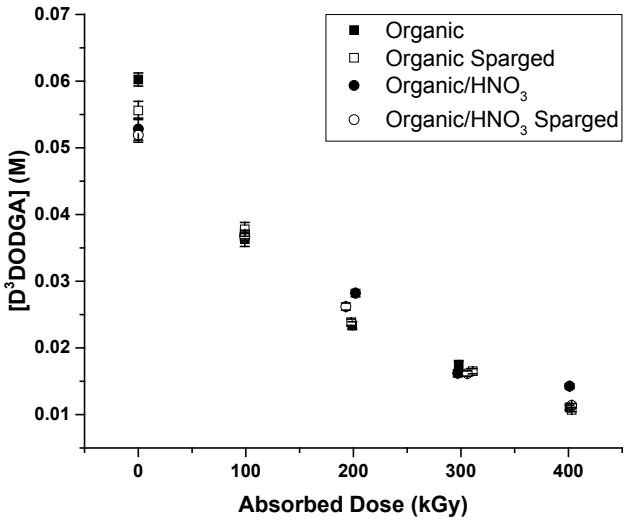

Figure 2: D^3DODGA concentration vs. absorbed dose. The unirradiated solutions are nominally 0.05 M D^3DODGA in *n*-dodecane. The solid squares are D^3DODGA organic phase; the open squares are D^3DODGA air sparged organic phase; the solid circles are the D^3DODGA organic phase contacted with 2.5 M HNO_3; the open circles are the D^3DODGA air sparged organic phase contacted with 2.5 M HNO_3. Each point is the mean of five measurements and the error bars represent 99% confidence intervals.

Table 1: Measured dose constants for the degradation of D^3DODGA in the four systems studied. The dose constants were calculated from linear fits of plots of ln[D^3DODGA] vs. absorbed dose. The uncertainty in the dose constants are 99% confidence intervals.

Sample	Dose Constant *d* (kGy^{-1})
0.05 D^3DODGA Organic	(4.1 ± 0.3) × 10^{-3}
0.05 D^3DODGA/2.5 M HNO_3	(3.4 ± 0.4) × 10^{-3}
Air Sparged 0.05 D^3DODGA Organic	(4.1 ± 0.3) × 10^{-3}
Air Sparged 0.05 D^3DODGA/2.5 M HNO_3	(3.9 ± 0.2) × 10^{-3}

Mean value	$(3.9 \pm 0.3) \times 10^{-3}$

Neither contact with the acidic aqueous phase nor the presence of sparged air had a significant effect on the radiolytic degradation rate of D^3DODGA. This is in agreement with the work of Zarzana et al.[25] and others,[23,24] where two similar diglycolamide compounds (TODGA and T(EH)DGA) were analyzed and it was found that the free radicals generated during irradiation of both a mildly acidic and highly acidic aqueous phase, such as $^{\bullet}OH$, $^{\bullet}NO_3$ and/or $^{\bullet}NO_2$ radicals, were apparently not important for the degradation of the DGA species. Further, the lack of a dissolved oxygen effect indicates that $^{\bullet}H$ atom and/or solvated electrons are not important reactive species in this system, because these would be quenched in the presence of oxygen, resulting in different radiolysis rates and pathways. Given the low starting concentration of the DGA (0.05 M), direct radiolytic decomposition is also not likely significant; therefore, based on the process of elimination the most likely mechanism for radiological degradation would be by reaction with a direct radiolysis product of the diluent, *n*-dodecane. This was previously postulated by Sugo et al.[23] and Zarzana et al.,[25] and called the sensitization effect.

IDENTIFICATION OF D^3DODGA RADIOLYSIS PRODUCTS

A number of radiolysis products of D^3DODGA were identified by UHPLC with positive-mode ESI-MS detection. A superposition of representative ion chromatograms for the compounds detected in 0.05 M D^3DODGA/*n*-dodecane after absorbing 401 kGy is shown in Figure 3. Radiolysis products were identified by examining variation in compound signal as a function of dose, and by explicitly searching for ion signals that would correspond to structures that could be formed from the parent DGA through bond cleavage, followed by capping with various radicals ($^{\bullet}H$, $^{\bullet}CH_3$, $^{\bullet}OH$, etc.). Identification of radiolysis products was also guided by compounds identified in radiolysis studies of other DGA molecules.[25,26] Additionally, high resolution mass spectrometry after chemical separation of the radiolysis products using HPLC in the Jülich laboratories was used to calculate molecular formulas based

on measured exact mass. The measured *m/z* ratios and calculated *m/z* ratios of each compound based on the most abundant isotopes agreed well (Supplementary Information, Table S2); deviations of the measured from the calculated *m/z* ratio were smaller than 1 ppm. The compounds detected by both laboratories using ESI and APCI were in good agreement. Proposed structures for the identified compounds, based on logical bond cleavage followed by capping that would result in the protonated and sodiated measured masses, along with the bond cleavages that would result in their formation are shown in Figure 4. Additional support for these structural assignments comes from collision-induced dissociation (CID) measurements.

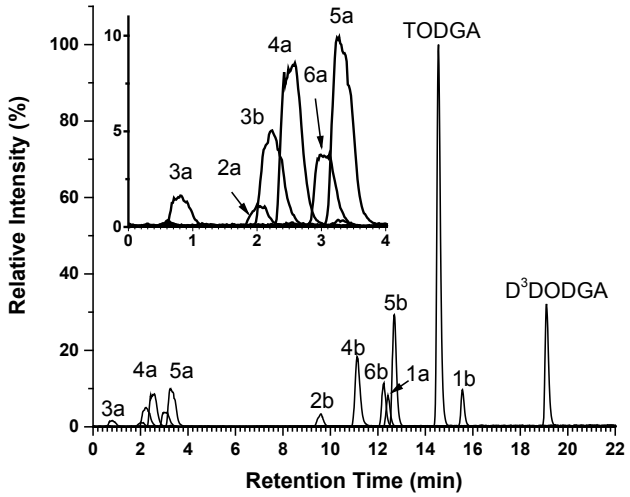

Figure 3: Overlaid ion chromatograms of 0.05 M D^{3}DODGA and its detected degradation products for irradiation of the D^{3}DODGA organic (no sparging or acid contact) to 401 kGy absorbed dose. The inset shows compounds 2a, 3a, 3b, 4a, 5a and 6a only. The *m/z* values for D^{3}DODGA and the degradation products all correspond to the respective protonated molecules, and are: 1a chromatogram *m/z* =, 525.5; 1b, 581.6; 2a, 358.3; 2b, 470.4; 3a, 242.3; 3b, 354.4; 4a, 300.3; 4b, 412.4; 5a, 284.3; 5b, 396.4; 6a, 270.3; 6b, 382.4;TODGA, 581.6; D^{3}DODGA, 693.7.

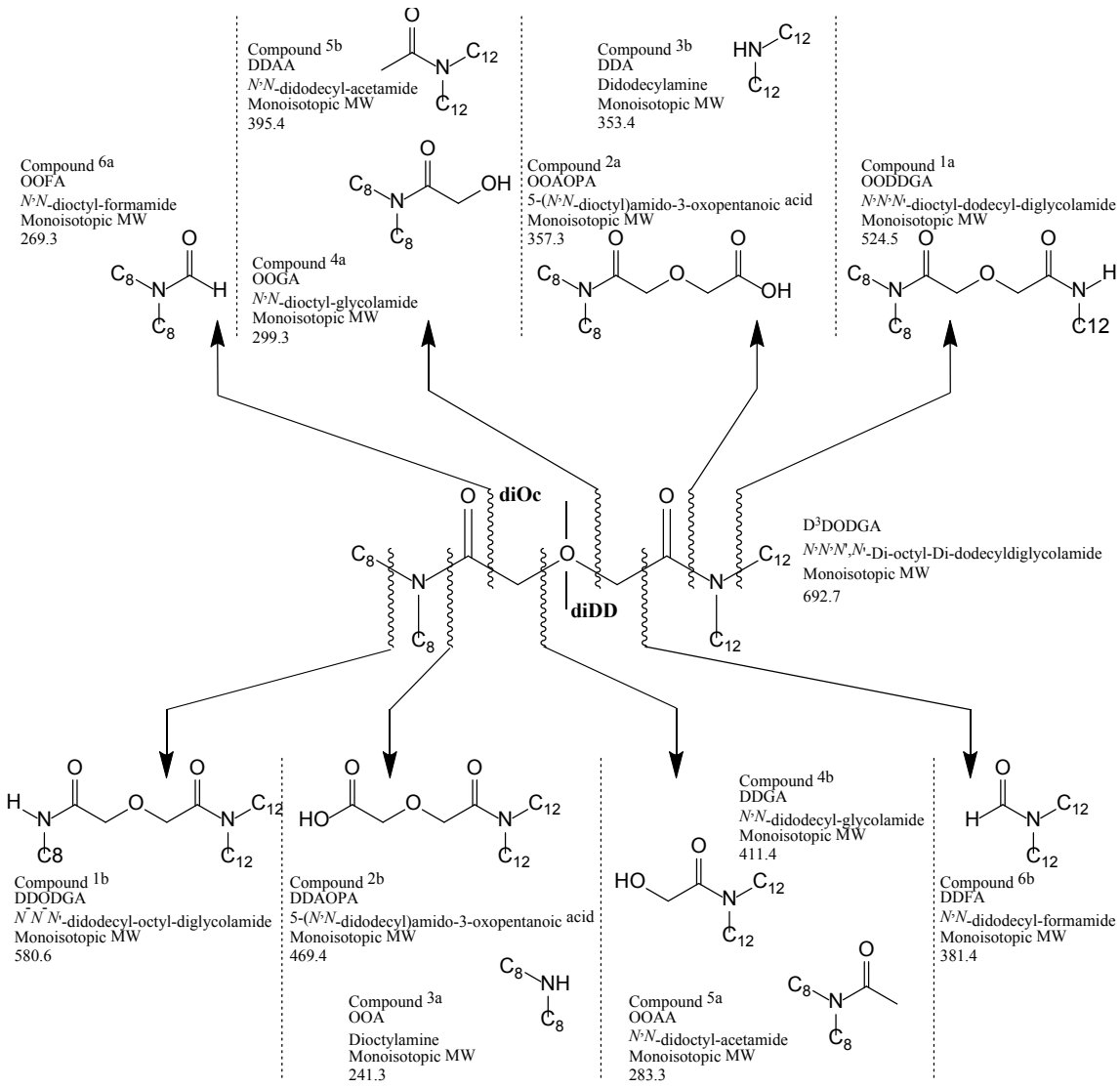

Figure 4: Proposed structures for radiolysis products observed for D^{3}DODGA with positive-mode ESI-MS, where C_8 is C_8H_{17} and C_{12} is $C_{12}H_{25}$.

Ionization using ESI and APCI generally produces intact, protonated species, and while high-resolution mass spectrometry can yield an unambiguous molecular formula, there is no structural information contained in the mass spectrum. Collision-induced dissociation (CID) measurements can be used to obtain some structural information by fragmenting precursor ions in the gas-phase and examining the ions that are produced. Briefly, the precursor ions are isolated using a mass analyzer after the ionization source (so no other ions are present) and then directed into a collision cell with a low pressure of neutral

gas. The isolated precursor ions are activated through low-energy collisions with the neutral gas, adding internal energy to the ions. The added energy is rapidly (on the order of femtoseconds) redistributed throughout all the vibrational modes of the precursor ion, causing the precursor ion to fragment into secondary ions that are then analyzed by mass spectrometry. The mass difference between the precursor and the detected secondary ions corresponds to neutral fragments lost by the precursor ion during fragmentation. These fragment ions and neutral losses can provide clues about the structure of the precursor.

D^3DODGA is expected to undergo radiolytic bond cleavage at every position along the DGA core: C_{alkyl}–N, N–$C_{carbonyl}$, $C_{carbonyl}$–CH_2, and CH_2–O_{ether}. Since D^3DODGA is non-symmetrical (one side, designated diOc, contains two *N*-octyl moieties, while the other, designated diDD, contains two *N*-dodecyl moieties), there are two variants for each of the bond cleavage reactions. The naming scheme used in Figure 4 has been designed so that all the labels that include the letter "a" contain the *N*-octyl moieties and all the labels that contain the letter "b" contain the *N*-didodecyl moieties.

Examination of the CID spectrum of the protonated parent DGA reveals fragmentation patterns that can be used to identify the structure of radiolysis products. The CID spectrum of D^3DODGA (Figure 5a) is dominated by two pairs of peaks at *m/z* = 452.4 and 424.4, and 340.3 and 312.3. These two groups can be explained as arising from similar fragmentation mechanisms on each side of the unsymmetric DGA molecule. Scheme I illustrates proposed fragmentation mechanisms and ion and neutral fragment structures for fragmentations occurring on the dioctyl side of D^3DODGA that would result in peaks at *m/z* = 452.4 and 424.4. Cleavage of the N–$C_{carbonyl}$ bond on the dioctyl side of D^3DODGA followed by a hydrogen transfer to the nitrogen (Scheme Ia) results in loss of neutral dioctyl amine and the formation of the ion at *m/z* = 452.4. Cleavage of the $C_{carbonly}$–CH_2 bond followed by a hydrogen transfer (Scheme Ib) would result in elimination of neutral dioctyl formamide and the formation of the ion at *m/z*=424.4. Similar cleavages on the didodecyl side of D^3DODGA would form ions with *m/z*=340.3 and 312.3.

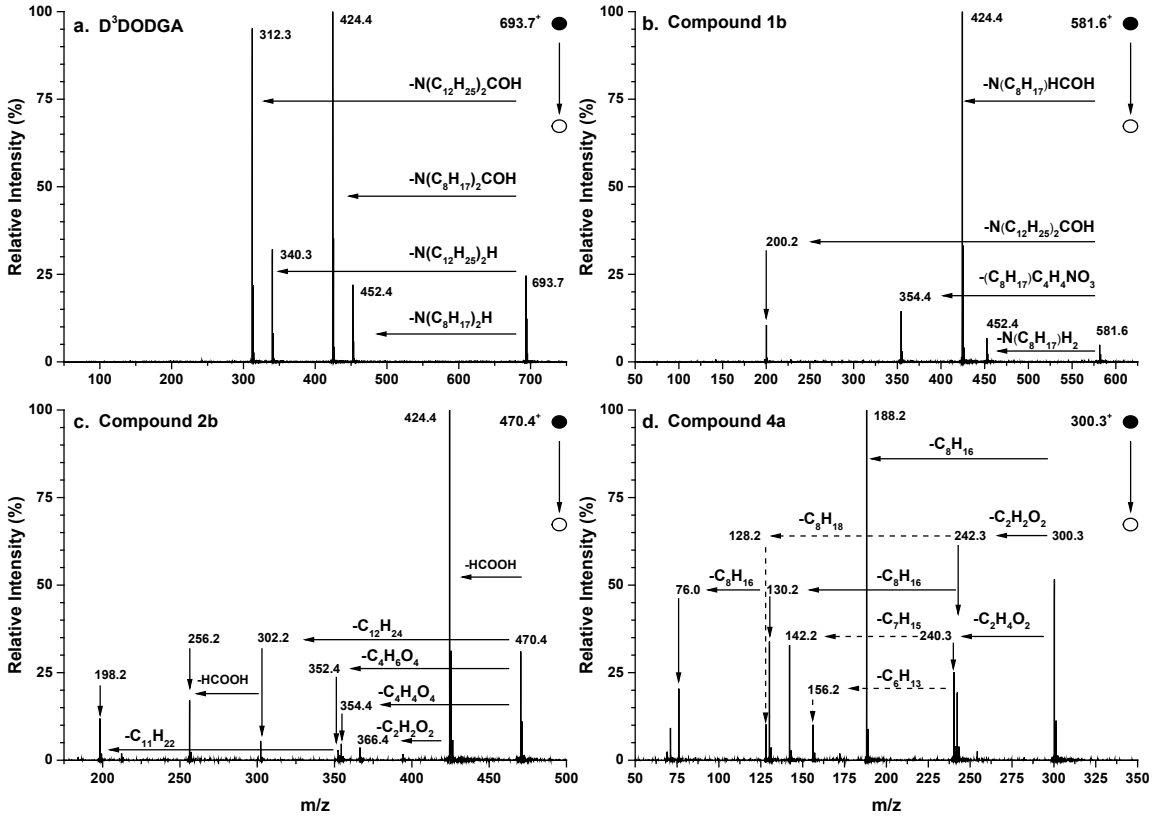

Figure 5: Collision-induced dissociation (CID) mass spectra of a) D^{3}DODGA, b) Compound 1a, c) Compound 2b, and d) Compound 4a. Horizontal arrows with neutral loss formulae represent proposed ion fragmentation pathways.

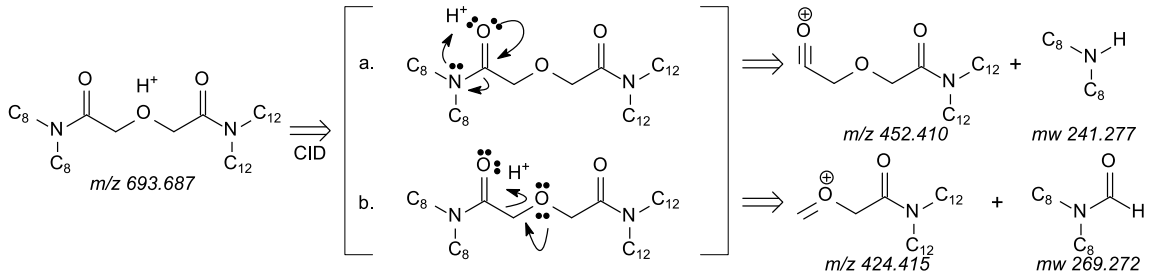

Scheme I: Proposed structures and fragmentation mechanisms for the ions at *m/z* = 452.4 and 424.4 in the CID spectrum of D^{3}DODGA.

The CID spectra of Compounds 1a and 1b are consistent with structures resulting from the radiolytic elimination of the dodecyl and octyl side chains, respectively. The CID reactions of Compound 1b

(Figure 4) are described in detail here, and we note that the CID reactions of Compound 1a are directly analogous. The mass spectrum of Compound 1b has a base peak at *m/z* = 581.5, assigned as [M+H$^+$] and a secondary peak 22 mass units higher at 603.5, assigned to [M+Na$^+$]. The monoisotopic molecular weight of 1a is thus 580.5 g/mol, which is 112.1 g/mol less than D^{3}DODGA, consistent with radiolytic cleavage of a C_{octyl}–N bond on the diOc side of D^{3}DODGA followed by hydrogen capping. This strongly suggests that 1b is *N,N,N'*-didodecyl-octyl-diglycolamide (DDOGA). The other product of this cleavage would be octane, but this compound lacks the ability to accept a proton, and so will not be observed in the UHPLC-ESI-MS analysis.

The CID spectrum of compound 1b (Figure 5b) supports this structural assignment. This spectrum contains three peaks (*m/z* = 452.4, 424.4, and 200.2) which would be formed from fragmentation mechanisms similar to those in Scheme I: *m/z* = 452.4 and 424.4 from cleavage of the N–$C_{carbonly}$ and $C_{carbonly}$–CH_2 bonds respectively on the now mono-Oc side of the molecule, forming the same ions seen in the D^{3}DODGA CID spectrum, and *m/z* = 200.2 from cleavage of the $C_{carbonly}$–CH_2 bond on the diDD side of the molecule, forming an ion 112.2 mass units lighter than the ion at *m/*z = 312.3 in the D^{3}DODGA CID spectrum. Interestingly, there is no peak at *m/z* = 228.2, which would arise from cleavage of N–$C_{carbonyl}$ bond on the diDD side of D^{3}DODGA and loss of the neutral didodecyl amine. There is, however, a peak at *m/z* = 354.4, which would correspond to the protonated didodecylamine, and elimination of a neutral molecule with a molecular weight of 227.1. We hypothesize the protonated amines arise from a molecular rearrangement mechanism, shown in Scheme II. There is no direct evidence for the structure of either the detected ion or the eliminated neutral, but the hypothetical structures shown in Scheme II would be expected to be stable. Protonated dioctylamine and protonated didodecylamine are observed in the CID spectra of the de-alkylated compounds 1a (peak at *m/*z = 242.2 in Supplementary Information Figure S1a), and 1b, respectively (peak at *m/z* = 354.4 in Figure 5b). Protonated didodecylamine is also seen in the CID spectrum of the acidic compound 2b (*m/z* 354.4 in Figure 5c). Curiously, the protonated amines are *not* seen in the CID spectrum of protonated D^{3}DODGA. The difference may lie in the fact that the intact DGA lacks a second mobile proton, which is available in

the aforementioned degradation products 1a, 1b, and 2b. We hypothesize that the fragmentation mechanism proposed in Scheme II is kinetically much faster than the cleavage of the N–$C_{carbonyl}$ bond depicted in Scheme I when there is a second mobile proton on the opposite side of the molecule from the N–$C_{carbonyl}$ bond.

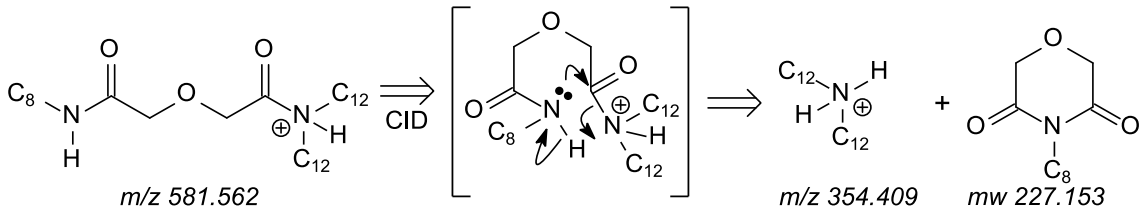

Scheme II: Proposed structures and fragmentation mechanism for the ion at *m/z* = 354.4 in the CID spectrum of Compound 1b.

Cleavage of the N–$C_{carbonyl}$ (amide) bond on the diOc side with H atom capping of the dangling bonds would be expected to form dioctylamine, and the corresponding aldehyde 5-(*N*,*N*-di(dodecyl)amido)-3-oxopentanal. The aldehyde derivative would have a high proton affinity and should readily produce abundant protonated and sodiated ions at *m/z* 454.4 and 476.4 respectively, but these are not observed; therefore, we conclude that the aldehyde is not formed. Instead, a chromatographic peak, Compound 2b, with a mass spectrum characterized by *m/z* 470.4 and 492.4 is observed: separated by 22 mass units, these probably represent protonated and sodiated versions of the same molecule. This suggests that in this cleavage, the dangling bond at the carbonyl is capped by a hydroxyl radical, forming 5-(*N*,*N*-di(dodecyl)amido)-3-oxopentanoic acid, which would have a molecular weight of 469.4 g mol^{-1}, and would furnish the protonated and sodiated ions seen.

The CID spectrum of Compound 2b (Figure 5c) has a base peak at 424.4, which is a loss of 46.0 mass units, or HCOOH, from the precursor ion (*m/z* = 470.4). This would correspond to gas-phase cleavage of the $C_{carbonyl}$–CH_2 bond followed by H capping on the diOc side of the proposed structure of Compound 2b, with elimination of neutral formic acid. The peak at *m/z* = 354.4 corresponds to the protonated didodecylamine, which could be formed by a mechanism hypothesized to be similar to that depicted in

Scheme II. Elimination of a $C_{12}H_{24}$ group (loss of 168.1 mass units) would yield the ion at *m/z* = 302.2, and a subsequent loss of formic acid (via the same mechanism that produced *m/z* = 424.4) would yield the ion at *m/z* = 256.2. The peak at *m/z* = 352.4 represents a new fragmentation pattern, *viz.* formation of an ion at 2 mass units below the protonated amine. We hypothesize this ion is the *N*-dodecyldodecanimine cation, formed by the mechanism proposed in Scheme III.

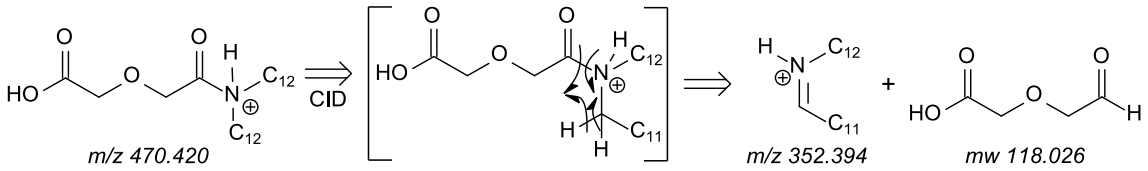

Scheme III: Proposed structures and fragmentation mechanism for the ion at *m/z* = 352.4 in the CID spectrum of Compound 2b.

The other product of radiolytic cleavage of the N–$C_{carbonyl}$ (amide) bond on the diOc side would be dioctylamine, with a molecular weight of 241.2. A chromatographic peak (Compound 3a) is observed with a mass spectrum with a dominant ion at *m/z* 242.2 ([M+H^+]), indicating a monoisotopic molecular mass of 241.2. The odd value for the monoisotopic molecular weight is consistent with a composition containing an odd number of nitrogen atoms, in accordance with the nitrogen rule. The CID spectrum of Compound 3a (Supplementary Information, Figure S2a) shows a peak corresponding to the loss of a C_8H_{16} group, consistent with the structural assignment of dioctylamine. The elemental composition of the compound was identified by accurate mass measurement using high resolution mass spectrometry.

The third type of expected radiolytic cleavage involves the $C_{carbonyl}$–CH_2 bonds. Rupture on the diOc side followed by H atom capping would be expected to generate two products, *N*,*N*-dioctylformamide (OOFA), and *N*,*N*-didodecyl-2-methoxyacetamide. Dioctylformamide has a molecular weight of 269 g/mol, and should generate protonated and sodiated ions at *m/z* 270 and 292, which are observed in the mass spectrum of Compound 6a eluting at 3.5 min. Radiolytic cleavage of the $C_{carbonyl}$–CH_2 bond on the diDD side should generate didodecylformamide (DDFA), with a molecular weight of 381, and protonated and sodiated ions at *m/z* 382 and 404 seen in the mass spectrum of Compound 6b eluting at 12.3 min.

The CID spectrum of Compound 6b (Supplementary Information, Figure S2e) shows loss of $C_{12}H_{24}$, which would be expected from the fragmentation of didodecylformamide. The other product would be *N*,*N*-dioctyl-2-methoxyacetamide; however, neither of the methoxyacetamide derivatives are observed. Peaks with very low signal intensity were assigned as *N*,*N*-dioctyl-2-methoxyacetamide and *N*,*N*-di(2-ethylhexyl)-2-methoxyacetamide in the analysis of TODGA and T(EH)DGA[25] but no methoxyacetamide products were observed for the methylated TODGA derivatives.[26] Because the formamide products are observed for all five DGAs we have studied (TODGA, T(EH)DGA, MeTODGA, Me_2TODGA, and D^3DODGA), it is likely this bond cleavage occurs. Therefore, it is unclear if the methoxyacetamide products are formed as a result of this cleavage, but at levels below the detection limit, or if the cleavage leads to formation of an alternative compound instead.

Finally, cleavage of the $C–O_{ether}$ bond on the diDD side followed by H atom capping of the dangling bonds would produce two compounds: *N*,*N*-dioctyl glycolamide, with a monoisotopic molecular mass of 299.3 g/mol, and *N*,*N*-di(dodecyl)acetamide, with a monoisotopic molecular mass of 395.4 g/mol. The CID spectrum of Compound 4a ($[M+H^+]$ = 299.3, Figure 5d) has a base peak at *m/z* = 188.2, which would arise from elimination of a C_8 olefin from one of the octyl side-chains of *N*,*N*-dioctyl glycolamide. The fragment ions at *m/*z = 242.3 and *m/z* = 240.3 are hypothesized to correspond to the protonated dioctylamine and the octyloctanimine cations, formed from protonated *N*,*N*-dioctyl glycolamide by mechanisms similar to those depicted in Scheme II and Scheme III, respectively. Additionally, each of these ions could fragment to form other peaks found in the CID spectrum. For example, the peaks at *m/z* = 156.2 and 142.2 could come from two different McLafferty rearrangements[32] of the octyloctanimine cation depicted in Scheme IV, further supporting this structural assignment. The other expected radiolytic product of the cleavage of the $C–O_{ether}$ bond on the diDD side of D^3DODGA would be didodecylacetamide, which would have a monoisotopic molecular mass of 395.4, the same as Compound 5b. The CID spectrum of Compound 5b (Supplementary Information, Figure S2d), shows a peak corresponding to protonated didodecyl amine (*m/z* = 354.4), and a peak corresponding to loss of a $C_{12}H_{24}$ side-chain (*m/z* = 228.2), suggesting Compound 5b is didodecylacetamide. The proposed structures for

Compounds 1a, 3b, and 5a are based on the above arguments using logical cleavages and capping, monoisotopic molecular weight, and CID data (SI, Figures S1 and S2).

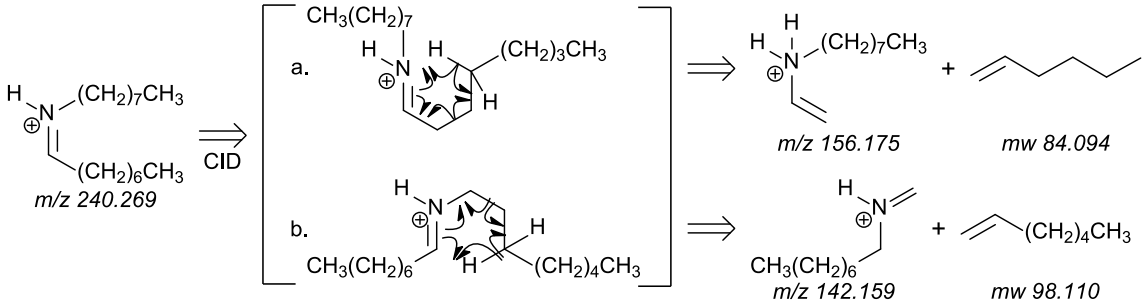

Scheme IV: Proposed structures and fragmentation mechanisms for the ions at *m/z* = 156.2 and 142.2 in the CID spectrum of Compound 4a.

Several other compounds were detected that appear to be related to the D[3]DODGA radiolysis (their signal increases with absorbed dose), but are unlikely to be primary radiolysis products. The first compound (Compound 2c, Supplementary Information, Figure S3) has a chromatographic peak with ions at *m/z* = 526 and 548 (indicating a protonated-sodiated pair), so the neutral molecular mass is likely 525, with a formula of $C_{32}H_{65}NO_4$ (Supplementary Information, Table S2). The dodecyl ester of Compound 2a would have a molecular formula matching this. The CID fragmentation spectrum (Supplementary information, Figure S4a) shows loss of 168 ($C_{12}H_{24}$), which is consistent with cleavage of the ester–$C_{12}H_{25}$ bond. The ion at *m/z* = 312 in the CID spectrum could be formed from cleavage of the DGA C–O_{ether} bond. This ion is seen in the CID spectra of D[3]DODGA and several degradation products with proposed structures with the C_8 side of the molecule intact. The ion at *m/z* = 312 could lose C_8H_{16} to form the ion at *m/z* = 200. Another compound, Compound 2d (*m/z* = 386, Supplementary Information, Table S2, Figure S3 and Figure S4b), has an exact formula and CID spectrum consistent with the ethyl-ester of Compound 2a. Both of these esters could be formed from a reaction between Compound 2a and the appropriate alcohol; however, source of the alcohols is unknown. The signals from both of these compounds are extremely low, so they could be the result of reactions of Compound 2a with alcohols present as contaminants in the diluent.

Two other detected compounds, Unknown 1 (*m/z* = 256) and Unknown 2 (*m/z* = 368), also have signals that increase with absorbed dose, especially for the acid contacted samples. Each has a peak 22 mass units higher with the same chromatographic profile when ionized using ESI, suggesting neutral formulas of $C_{16}H_{33}NO$ and $C_{24}H_{49}NO$ respectively. The CID spectra of these two compounds show loss of C_8H_{16} (Unknown 1) and $C_{16}H_{24}$ (Unknown 2), suggesting they are related to D^{3}DODGA, but the carbon/hydrogen ratio suggests part of each molecule is unsaturated. Unknown 1 is present in the unirradiated samples, so it could be a synthesis impurity that is also produced by radiolysis or hydrolysis. However, there is not enough information to draw conclusions about the identity of these compounds.

BEHAVIOR OF D^{3}DODGA RADIOLYSIS PRODUCTS AS A FUNCTION OF ABSORBED DOSE

The effects on solvent extraction separations due to these degradation products have not been thoroughly investigated. Núñez et al. reported on properties of selected TODGA degradation compounds and their effects on solvent extraction systems.[33] Acidic degradation compounds were found to possibly interfere with a selective back-extraction step in solvent extraction processes. Other degradation compounds showed increased co-extraction of fission products. Degradation compounds with 2-hydroxy-acetamide structure showed increased Mo extraction and other degradation compounds showed higher co-extraction of Zr and Pd. It was concluded that the degradation of TODGA would lead to an overall increased co-extraction of undesired fission products. However, based on analogy with TODGA and the solvent extraction ligand octylphenyl-*N*,*N*-diisobutylcarbamoylmethylphosphine oxide (CMPO), the production of acidic degradation products (such as DDAOPA and OOAOPA, Figure 4) may adversely affect stripping of the metal-loaded organic phase.[34,35] The concentration changes of the detected radiolysis products as a function of absorbed dose (Figure 6) can be examined based on the proposed structures. Compounds 1b and 2b (Figure 6a and Figure 6b, respectively) grow in as dose increases, indicating they are directly formed by radiolysis. The signal for Compound 1b peaks at about 300 kGy and the signal for Compound 2b peaks at about 200 kGy at which point the signal begins to decrease, indicating these

radiolysis products themselves are susceptible to radiolysis. Given the proposed structures, DDODGA and DDAOPA, this is not surprising, since these structures still have the C–O_{ether}, C–$C_{carbonyl}$ and N–$C_{carbonyl}$ bonds whose rupture is proposed to lead the other detected radiolysis products. The same behavior was observed by Galán et al.[26] for structurally comparable degradation compounds, which are believed to be formed through the same radiolysis mechanism. The acidic compound 2-((1-(dioctylamino)-1-oxopropan-2-yl)oxy)acetic acid (comparable to Compound 2a) and the single dealkylation compound (comparable to Compound 1a) showed the same increase in dose up to 200 – 300 kGy, after which the normalized intensity decreased. Compounds 5b and 6b (Figure 6c and Figure 6d, respectively) grow in as absorbed dose increases, consistent with their structural assignments as small radiolysis products.

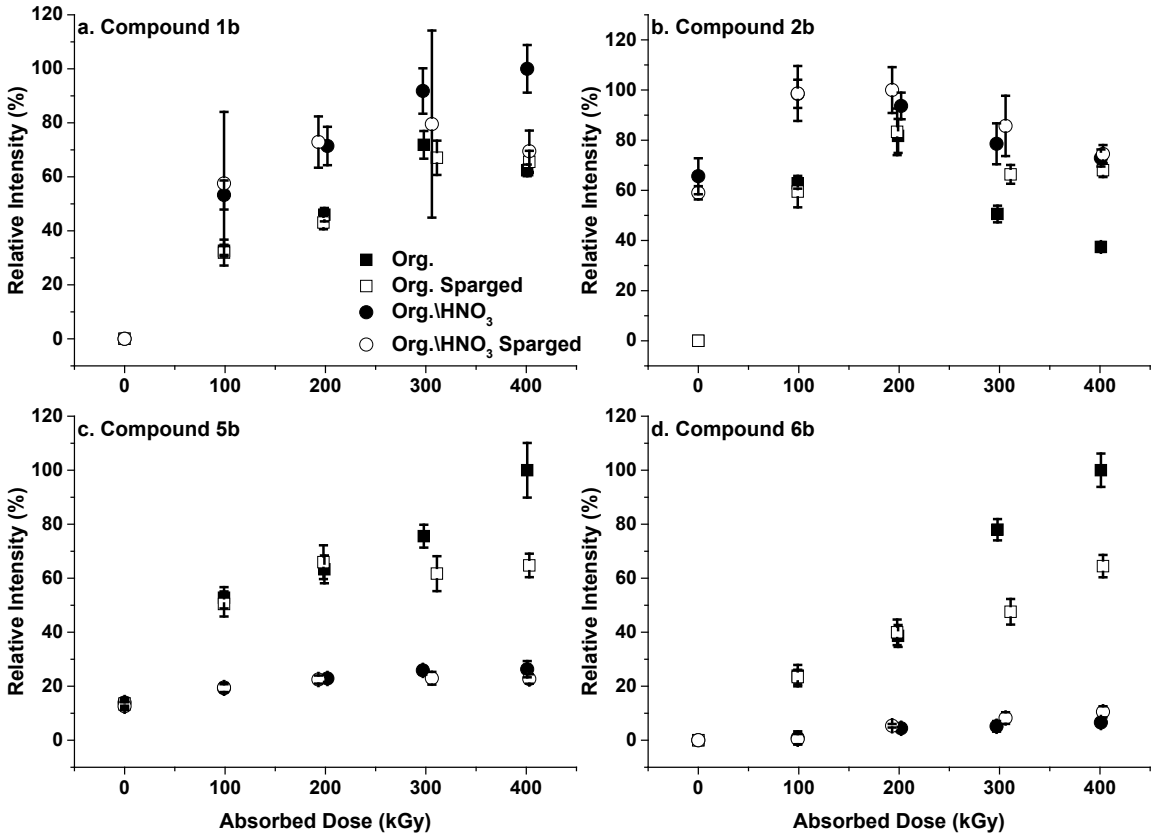

Figure 6: Normalized signal vs. absorbed dose for degradation products 1b, 2b, 5b and 6b. The solid squares are 0.05 M D^{3}DODGA organic phase; the open squares are 0.05 M D^{3}DODGA air sparged organic phase; the solid circles are 0.05 M D^{3}DODGA organic phase contacted with 2.5 M HNO_3; the open circles are 0.05 M D^{3}DODGA air sparged organic phase contacted with 2.5 M HNO_3. Each point is the mean of five measurements and the error bars represent 99% confidence intervals.

The course of the radiolysis does appear to be affected, however, in the acid-contacted experiment compared to the non-acid-contacted experiment. After 100 kGy more of the de-alkylated, and de-aminated products are formed in the acid contacted experiments, and conversely, there is comparatively less of the products arising from radiolytic cleavage of the $C_{carbonyl}$–C and C–O_{ether} bonds. Acid contact clearly tends to favor cleavage at the nitrogen atoms, though this preference doesn't seem to affect the overall degradation rate. We hypothesize that the presence of acid results in amide functional groups that

are at least partially protonated, resulting in weakening of the N–C_{alkyl} and N–$C_{carbonyl}$ bonds relative to the C–$C_{carbonyl}$ and C–O_{ether} bonds. The primary degradation products formed in the presence of the acidic aqueous phase will have high metal coordination complex formation constants. These degradation products could decrease the distribution ratios of an extraction if they have aqueous solubility, and could impede stripping if they remain in the organic phase. In contrast, in the non-acid-contacted experiments there is a greater rate of formation of products in which the DGA core is broken, which would not be expected to be effective extractants.

7. Conclusions

The results of this study suggest that there is no difference between the rate of γ-radiolysis of D^3DODGA and those of TODGA and T(EH)DGA. Additionally, the rate appears to be unaffected by contact with nitric acid and air sparging, providing additional evidence that radical cations produced in the alkane diluent are the reactive species initiating decomposition. There does seem to be a difference in degradation chemistry that depends on whether the organic phase is in contact with acid; in the presence of an acidic aqueous phase, the preferred site for radiolytic attack appears to be at the amide nitrogen atoms, which produces a higher fraction of products generated from rupture of the N–$C_{carbonyl}$ and the N–C_{alkyl} bonds. The C–O_{ether} and C–$C_{carbonyl}$ bonds are also broken, but these reactions account for a greater fraction of the overall reactivity in the non-acid-contacted experiments. Thus, a study of the effect of the potentially more deleterious radiolysis products generated in the presence of the acidic aqueous phase on solvent extraction performance is warranted.

There is also a striking similarity in the degradation pathway of D^3DODGA when compared to the degradation of TODGA, T(EH)DGA, MeTODGA and Me_2TODGA.[24,25] The similarity in degradation rates of these DGA compounds, along with the identified radiolysis products discussed above, strongly suggests that the diglycolamide center of these molecules, not the side-chains, is most vulnerable to radiolytic degradation, apparently all by reaction with a common species produced by radiolysis of the diluent.

8. Acknowledgements

The gamma-ray irradiation and UHPLC-ESI MS experiments performed at Idaho National Laboratory were supported by the US Department of Energy (US-DOE), Assistant Secretary for Nuclear Energy, under the Fuel Cycle R&D Program, Idaho Operations Office Contract DE-AC07-05ID14517. Additional financial support for this research was provided by the European Commission (projects SACSESS – Contract No. FP7-Fission-2012-323-282).

9. References

1. Todd, T. A. Separation Research for Advanced Nuclear Fuel Cycles. In *Nuclear Energy and the Environment*; Wai, C. M., Mincher, B. J., Eds.; American Chemical Society: Washington, D.C., 2010; pp 13–18.
2. Hudson, M. J.; Harwood, L. M.; Laventine, D. M.; Lewis, F. W. Use of Soft Heterocyclic N-Donor Ligands to Separate Actinides and Lanthanides. Inorg. Chem. **2013**, *52* (7), 3414–3428.
3. Madic, C.; Lecomte, M.; Baron, P.; Boullis, B. Separation of Long-Lived Radionuclides from High Active Nuclear Waste. Comptes Rendus Physique **2002**, *3* (7–8), 797–811.
4. Magill, J.; Berthou, V.; Haas, D.; Galy, J.; Schenkel, R.; Wiese, H.-W.; Heusener, G.; Tommasi, J.; Youinou, G. Impact Limits of Partitioning and Transmutation Scenarios on the Radiotoxicity of Actinides in Radioactive Waste. Nuclear Energy **2003**, *42* (5), 263–277.
5. Ansari, S. A.; Pathak, P.; Mohapatra, P. K.; Manchanda, V. K. Chemistry of Diglycolamides: Promising Extractants for Actinide Partitioning. Chem. Rev. **2012**, *112* (3), 1751–1772.
6. Ansari, S. A.; Pathak, P.; Mohapatra, P. K.; Manchanda, V. K. Aqueous Partitioning of Minor Actinides by Different Processes. Separation & Purification Reviews **2011**, *40* (1), 43–76.
7. Sasaki, Y.; Sugo, Y.; Suzuki, S.; Tachimori, S. The Novel Extractants, Diglycolamides, for the Extraction of Lanthanides and Actinides in HNO_3–*n*-Dodecane System. Solvent Extr. Ion Exch. **2001**, *19* (1), 91–103.
8. Mowafy, E. A.; Aly, H. F. Synthesis of Some *N*,*N*,*N*′,*N*′-Tetraalkyl-3-Oxa-Pentane-1,5-Diamide and Their Applications in Solvent Extraction. Solvent Extr. Ion Exch. **2007**, *25* (2), 205–224.
9. Tachimori, S.; Sasaki, Y.; Suzuki, S. Modification of TODGA-*N*-Dodecane Solvent with a Monoamide for High Loading of Lanthanides(III) and Actinides(III). Solvent Extr. Ion Exch. **2002**, *20* (6), 687–699.
10. Sasaki, Y.; Sugo, Y.; Suzuki, S.; Kimura, T. A Method for the Determination of Extraction Capacity and Its Application to *N*,*N*,*N*′,*N*′-Tetraalkylderivatives of Diglycolamide-Monoamide/n-Dodecane Media. Anal. Chim. Acta **2005**, *543* (1–2), 31–37.
11. Sasaki, Y.; Zhu, Z.-X.; Sugo, Y.; Suzuki, H.; Kimura, T. Extraction Capacity of Diglycolamide Derivatives for Ca(II), Nd(III) and Zr(IV) from Nitric Acid to *n*-Dodecane Containing a Solvent Modifier. Anal. Sci. **2005**, *21* (10), 1171–1175.
12. Modolo, G.; Asp, H.; Schreinemachers, C.; Vijgen, H. Development of a TODGA Based Process for Partitioning of Actinides from a PUREX Raffinate Part I: Batch Extraction Optimization Studies and Stability Tests. Solvent Extr. Ion Exch. **2007**, *25* (6), 703–721.
13. Modolo, G.; Asp, H.; Vijgen, H.; Malmbeck, R.; Magnusson, D.; Sorel, C. Demonstration of a TODGA-Based Continuous Counter-Current Extraction Process for the Partitioning of Actinides from a Simulated PUREX Raffinate, Part II: Centrifugal Contactor Runs. Solvent Extr. Ion Exch. **2007**, *26* (1), 62–76.
14. Magnusson, D.; Christiansen, B.; Glatz, J.; Malmbeck, R.; Modolo, G.; Serrano-Purroy, D.; Sorel, C. Demonstration of a TODGA Based Extraction Process for the Partitioning of Minor Actinides from a PUREX Raffinate. Solvent Extr. Ion Exch. **2009**, *27* (1), 26–35.
15. Ravi, J.; Suneesh, A. S.; Prathibha, T.; Venkatesan, K. A.; Antony, M. P.; Srinivasan, T. G.; Vasudeva Rao, P. R. Extraction Behavior of Some Actinides and Fission Products from Nitric Acid Medium by a New Unsymmetrical Diglycolamide. Solvent Extr. Ion Exch. **2011**, *29* (1), 86–105.
16. Ravi, J.; Venkatesan, K. A.; Antony, M. P.; Srinivasan, T. G.; Vasudeva Rao, P. R. Tuning the Diglycolamides for Modifier-Free Minor Actinide Partitioning. J. Radioanal. Nucl. Chem. **2013**, *295* (2), 1283–1292.
17. Ravi, J.; Venkatesan, K. A.; Antony, M. P.; Srinivasan, T. G.; Vasudeva Rao, P. R. Feasibility of Using Di-Dodecyl-Di-Octyl Diglycolamide for Partitioning of Minor Actinides from Fast Reactor High-Level Liquid Waste. Solvent Extr. Ion Exch. **2014**, *32* (4), 424–436.

18. Nayak P. K.; Kumaresan R.; Chaurasia Shivkumar; Venkatesan K. A.; Subramanian G. G. S.; Prathibha T.; Syamala K. V.; Selvan B. Robert; Rajeswari S.; Antony M. P.; et al. Studies on the Feasibility of Using Completely Incinerable Reagents for the Single-Cycle Separation of Americium(III) from Simulated High-Level Liquid Waste. Radiochim. Acta **2014**, *103* (4), 265.
19. Nayak P. K.; Kumaresan R.; Chaurasia Shivkumar; Venkatesan K. A.; Subramanian G. G. S.; Rajeswari S.; Antony M. P.; Vasudeva Rao P. R.; Bhanage B. M. Demonstration of Trivalent Actinide Partitioning from Simulated High-Level Liquid Waste Using Modifier-Free Unsymmetrical Diglycolamide in *N*-Dodecane. Radiochim. Acta **2015**, *103* (5), 359.
20. Ravi Jammu; Venkatesan K. A.; Antony M. P.; Srinivasan T. G.; Vasudeva Rao P. R. New Unsymmetrical Digycolamide Ligands for Trivalent Actinide Separation. Radiochim. Acta **2014**, *102* (7), 609.
21. Sypula, M.; Wilden, A.; Schreinemachers, C.; Malmbeck, R.; Geist, A.; Taylor, R.; Modolo, G. Use of Polyaminocarboxylic Acids as Hydrophilic Masking Agents for Fission Products in Actinide Partitioning Processes. Solvent Extr. Ion Exch. **2012**, *30* (7), 748–764.
22. Sugo, Y.; Sasaki, Y.; Tachimori, S. Studies on Hydrolysis and Radiolysis of *N*,*N*,*N'*,*N'*-Tetraoctyl-3-Oxapentane-I,5-Diamide. Radiochim. Acta **2002**, *90*, 161–165.
23. Sugo, Y.; Izumi, Y.; Yoshida, Y.; Nishijima, S.; Sasaki, Y.; Kimura, T.; Sekine, T.; Kudo, H. Influence of Diluent on Radiolysis of Amides in Organic Solution. Radiat. Phys. Chem. **2007**, *76*, 794–800.
24. Galán, H.; Núñez, A.; Espartero, A. G.; Sedano, R.; Durana, A.; Mendoza, J. de. Radiolytic Stability of TODGA: Characterization of Degraded Samples under Different Experimental Conditions. Procedia Chem. **2012**, *7* (0), 195–201.
25. Zarzana, C. A.; Groenewold, G. S.; Mincher, B. J.; Mezyk, S. P.; Wilden, A.; Schmidt, H.; Modolo, G.; Wishart, J. F.; Cook, A. R. A Comparison of the γ-Radiolysis of TODGA and T(EH)DGA Using UHPLC-ESI-MS Analysis. Solvent Extr. Ion Exch. **2015**, *33* (5), 431–447.
26. Galán, H.; Zarzana, C. A.; Wilden, A.; Nunez, A.; Schmidt, H.; Egberink, R. J. M.; Leoncini, A.; Cobos, J.; Verboom, W.; Modolo, G.; et al. Gamma-Radiolytic Stability of New Methylated TODGA Derivatives for Minor Actinide Recycling. Dalton Trans. **2015**, *44* (41), 18049–18056.
27. Mincher, B. J.; Modolo, G.; Mezyk, S. P. Review Article: The Effects of Radiation Chemistry on Solvent Extraction 3: A Review of Actinide and Lanthanide Extraction. Solvent Extr. Ion Exch. **2009**, *27* (5–6), 579–606.
28. Galán, H.; Murillo, M. T.; Sedano, R.; Núñez, A.; de Mendoza, J.; González-Espartero, A.; Prados, P. Hydrolysis and Radiation Stability of M-Xylylene Bis-Diglycolamide: Synthesis and Quantitative Study of Degradation Products by HPLC–APCI+. Eur. J. Org. Chem. **2011**, *2011* (20–21), 3959–3969.
29. Ravi Jammu; Selvan B. Robert; Venkatesan K. A.; Antony M. P.; Srinivasan T. G.; Vasudeva Rao P. R. Radiolytic Stability of Di-2-Ethylhexyl-Dioctyl Diglycolamide. Radiochim. Acta **2014**, *102* (5), 451.
30. Ravi, J.; Robert Selvan, B.; Venkatesan, K. A.; Antony, M. P.; Srinivasan, T. G.; Vasudeva Rao, P. R. Evaluation of Radiation Stability of *N*,*N*-Didodecyl *N'*,*N'*-Di-Octyl Diglycolamide: A Promising Reagent for Actinide Partitioning. J. Radioanal. Nucl. Chem. **2014**, *299* (1), 879–885.
31. Gujar, R. B.; Ansari, S. A.; Bhattacharyya, A.; Kanekar, A. S.; Pathak, P. N.; Mohapatra, P. K.; Manchanda, V. K. Radiolytic Stability of *N*,*N*,*N'*,*N'*-Tetraoctyl Diglycolamide (TODGA) in the Presence of Phase Modifiers Dissolved in N-Dodecane. Solvent Extr. Ion Exch. **2012**, *30* (3), 278–290.
32. McLafferty, F. W. 6.8 Amines. In *Interpretation of Mass Spectra*; W. A. Benjamin, Inc.: London, 1973; pp 156–163.
33. Núñez, A.; Galán, H.; Cobos, J. TODGA Degradation Compounds: Properties and Effects on Extraction Systems. In *Proceedings of GLOBAL 2015 Nuclear Fuel Cycle for a Low-Carbon Future*; Paris, France, 2015; p 1623–1630, Paper 5400.
34. Nash, K. L.; Gatrone, R. C.; Clark, G. A.; Rickert, P. G.; Horwitz, E. P. Hydrolytic and Radiolytic Degradation of Oφd(iB)Cmpo: Continuing Studies. Sep. Sci. Technol. **1988**, *23* (12–13), 1355–1372.

35. Mincher, B. J.; Mezyk, S. P.; Elias, G.; Groenewold, G. S.; Riddle, C. L.; Olson, L. G. The Radiation Chemistry of CMPO: Part 1. Gamma Radiolysis. Solvent Extr. Ion Exch. **2013**, *31* (7), 715–730.